

## STRUCTURAL HARDENING MECHANISM OF LEAD-CADMIUM-BISMUTH-TIN ALLOYS FOR BATTERY GRIDS

S. SAISSI<sup>1</sup>, K. MARBOUH<sup>1</sup>, L. ZERROUK<sup>1</sup>, A. IBNLFASSI<sup>1</sup>, A. JOURANI<sup>1</sup>,  
Y. AIT YASSINE<sup>2</sup>, L. BOURDEN<sup>2</sup>, M. RATTAL<sup>3</sup>, E. SAAD<sup>1</sup>

*Manuscript received: 12.01.2015; Accepted paper: 04.02.2015;*

*Published online: 30.03.2015.*

**Abstract.** *The phenomenon of aging and overaging of Pb-Cd-Bi-Sn alloys is characterized by a discontinuous processing and a continuous reaction, it's hardening and softening. The presence of tin slows kinetics of hardening transformation and increases the hardness.*

*Our study is devoted to determine precipitation type, nature and phase morphology of precipitates and the intensity of hardening in the quaternary alloys Pb-Cd-Bi-Sn. The return to equilibrium of supersaturated alloys Pb-Cd-Sn-Bi has been studied by different techniques: hardness, optical microscopy and X-ray diffraction. Two structural states were considered: raw casting alloy and rehomogenized alloy. The studied alloys are: Pb2% Cd1% Bi, Pb 2% Cd2% Bi, Pb 2% Cd3% Bi with different percentages of tin 0.25% Sn, 0.5% Sn, 1.25% Sn and 2% Sn. Experimental temperatures are 20 °C and 80 °C. Bismuth accelerates the hardening reaction, while tin has a retarding effect on the hardening process.*

**Keywords:** *Alloy, discontinuous precipitation, continuous reaction, hardening, softening, aging, over-aging, battery grids.*

### 1. INTRODUCTION

A systematic study of the ternary alloy Pb-Cd-Bi has been previously established by Saissi and all [2]. Aging of these alloys is characterized by a discontinuous processing and a hardening continuous reaction, while the overaging is characterized by a softening discontinuous precipitation.

Being a minor additive in battery grids, Tin is deemed efficient in mechanical and electrochemical properties [1], hence the idea to add it to our mother alloy and see its influence according to defined proportions. Our goal is to study systematically the process of aging and overaging of supersaturated soaked solutions for these alloys Pb-Cd-Bi-Sn by different techniques: hardness, optical microscopy and X-ray diffraction.

---

<sup>1</sup> University Hassan 1 FST Settat, Laboratory of Physicochemistry of Materials and Processes (MPCP), Morocco. E-mail: [saadelmadani73@gmail.com](mailto:saadelmadani73@gmail.com).

<sup>2</sup> Ibn Zohr University, Faculty of Science, Laboratory of Thermodynamics and energy, Agadir, Morocco.

<sup>3</sup> The Higher Institute of Health and Sciences, Settat, Morocco.

## 2. EXPERIMENTAL SETUP

### 2.1. PREPARATION OF ALLOYS

The alloys are prepared from pure metals: lead (99.99%), cadmium (99.99%), bismuth (99.99%) and tin (99.99%).

The three systems Pb-Cd [3], Pb-Sn [4] and Bi-Sn [6] have a simple eutectic diagram. In the ternary system Pb-Cd-Sn [5], only three solid phases are observed: Pb, Cd and Sn, as indicated in the isothermal sections of the ternary system at temperatures 130°C, 145°C and 180°C [5] of Figure 3.

For the binary phase diagram of Pb-Sn system [4], it has a eutectic at a temperature of 183 °C and a composition of 61.9 wt% Sn. The solubility of Sn in Pb at 183°C is about 19wt%, which decreases to a value which is not well known at room temperature (Figure 1). In the literature the concentrations by weight of tin is 1,9 [7], 2-3 [8], 1,3 [9], 1-2[10-11].

The concentrations by weight of tin chosen for the elaboration of these alloys are: 0.25% Sn, 0.5% Sn, 1.25% Sn and 2% Sn.

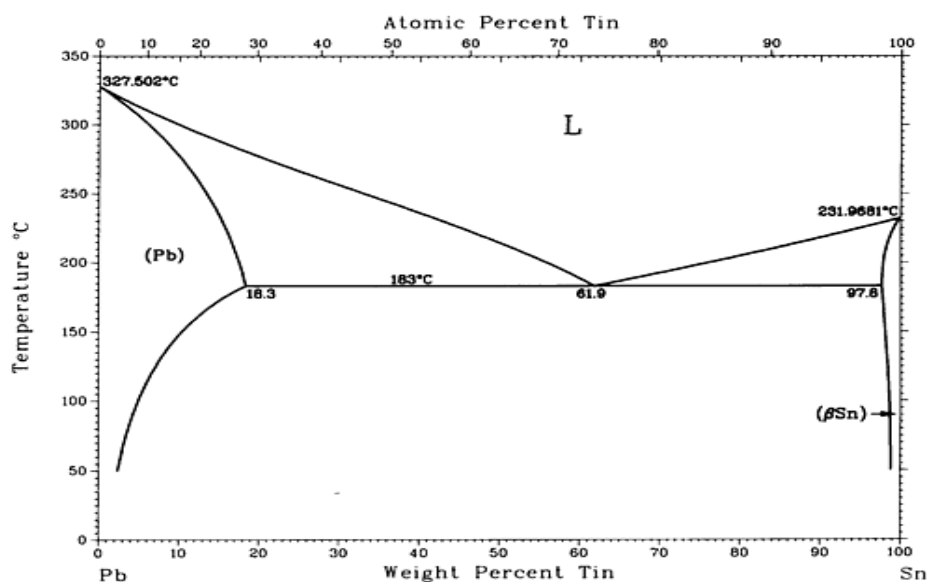


Fig. 1. Pb-Sn phase diagram [4].

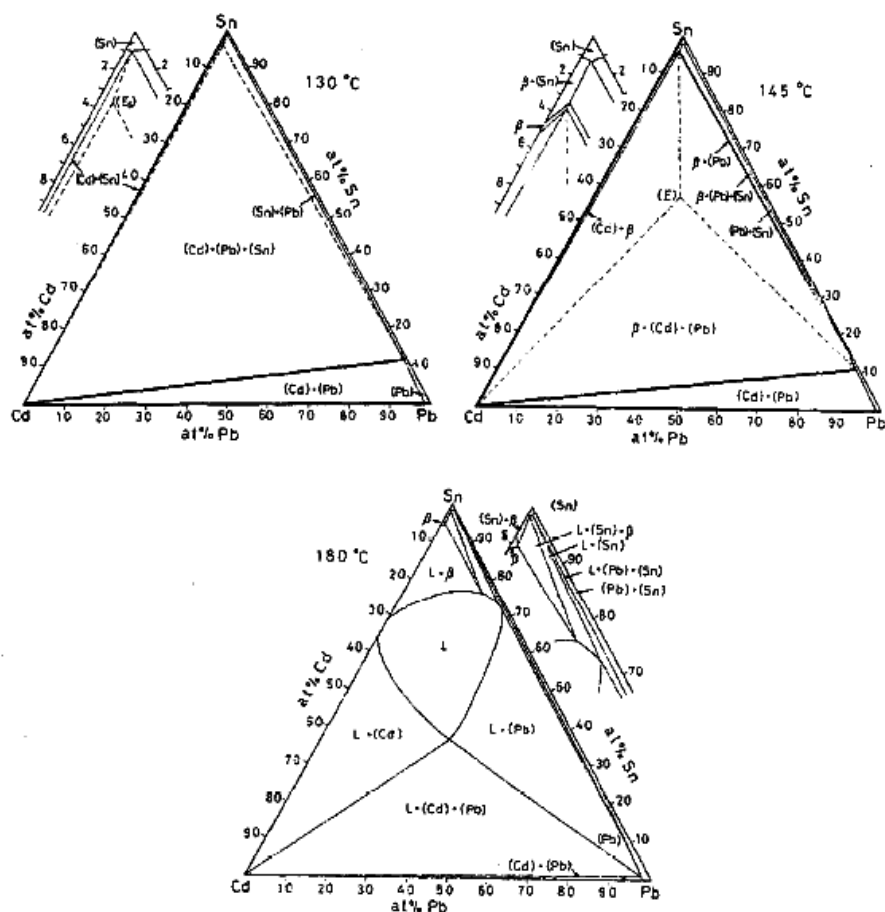


Fig. 2. Isothermal sections of the Pb-Cd-Sn system at 130°C, 145°C and 180°C [5].

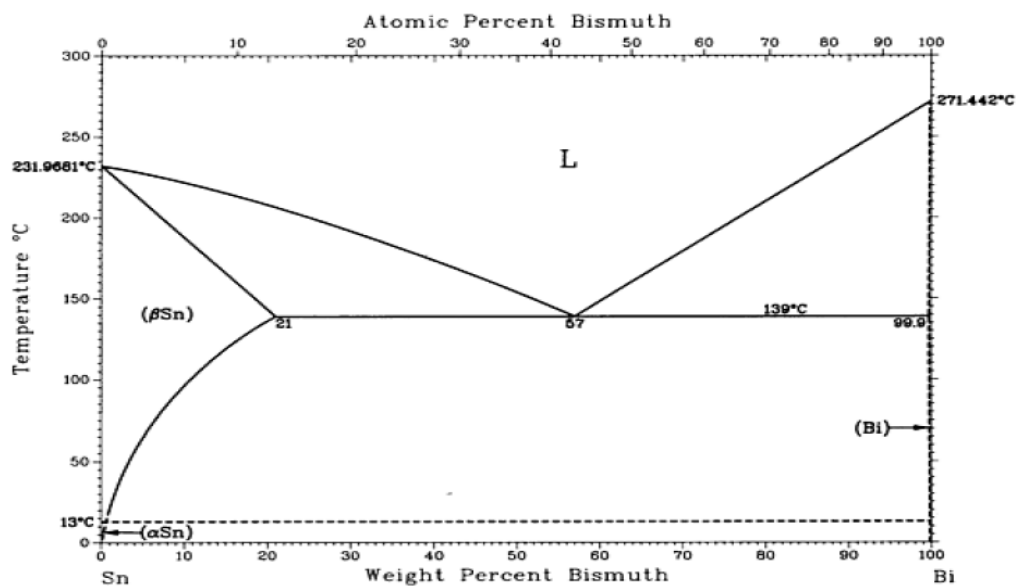


Fig. 3. Sn-Bi phase diagram [6].

We have developed alloys whose compositions are given in Table 1.

**Table 1. Composition of the studied alloys.**

weight content (%Cd)	weight content (%Bi)	weight content (%Sn)
2	1	0,5
2	1	2
2	2	0,25
		0,5
		1,25
		2
2	3	0,25
		0,5
		1,25
		2

To study the structural-cast alloys, the elements taken in the proper proportions, are introduced into a silica ampoule of 8 mm in diameter, sealed under high vacuum, the mixture is heated to 500°C. After melting and cooling total, the tube is quenched with water. The samples were examined directly or may be stored in liquid nitrogen. For rehomogenization, the ingot obtained is cut into several pieces that are then polished by abrasion. Samples are introduced into silica ampoules sealed under high vacuum. The whole is kept at 264 °C for 2 h (estimated optimal for rehomogenization) and then quenched with water.

## 2.2. HARDNESS

The hardness tests are carried out by the vickers method, using a durometer testweel under a load of 2Kgf. Each measurement is the average of up to five trucks spread over a flat section corresponds to a diametric plane or perpendicular to the axis of the cylindrical sample. The sections are obtained by sawing, mechanical abrasion and chemical polishing. Recall that the empirical relation  $HV = 0,3(R)$  can be used to evaluate the rupture strength (R) of these alloys.

## 2.3. TECHNICAL MICROGRAPHIC OBSERVATION

The physical properties of solid solutions for soaked lead alloys change from room temperature. The curing mechanisms correspond to continuous and / or discontinuous transformations. Indeed, this temperature corresponds to  $0.5 T_{\text{fusion}} (^{\circ}\text{K})$ , temperature at which the alloy elements can diffuse.

The observation of the structure of alloys corresponding to the continuous / discontinuous transformations is made by using the optical microscope, the samples must undergo mechanical polishing, chemical polishing using hydrogen peroxide 30%  $\text{H}_2\text{O}_2$  and three share of glacial acetic acid for 20 seconds to 2 minutes, then chemical attack using 100g of ammonium molybdate; 250g citric acid and water in sufficient quantity to have a liter of the mixture [12].

### 3. RESULTS

#### 3.1. STUDY OF THE ALLOY Pb2% Cd1% Bi0, 5% Sn:

##### 3.1.1. Hardness

Fig. 4 shows the change in hardness with time at 20°C of raw casting alloys Pb2%Cd1%Bi[2], and Pb2% Cd1% Bi0, 5% Sn. Both curves have the same shape, but we note that the influence of tin is manifested by an increase in hardness and a slowing of the hardening reaction. Indeed, in the absence of tin, the hardness is 11,125 HV after 6 minutes and culminates 12.53 HV after 80 minutes (maximum) of aging. In the presence of tin (0, 5% by weight), the hardness is 12,08 HV after 7 minutes and the maximum (about 13,23 HV) is obtained after 110 minutes.

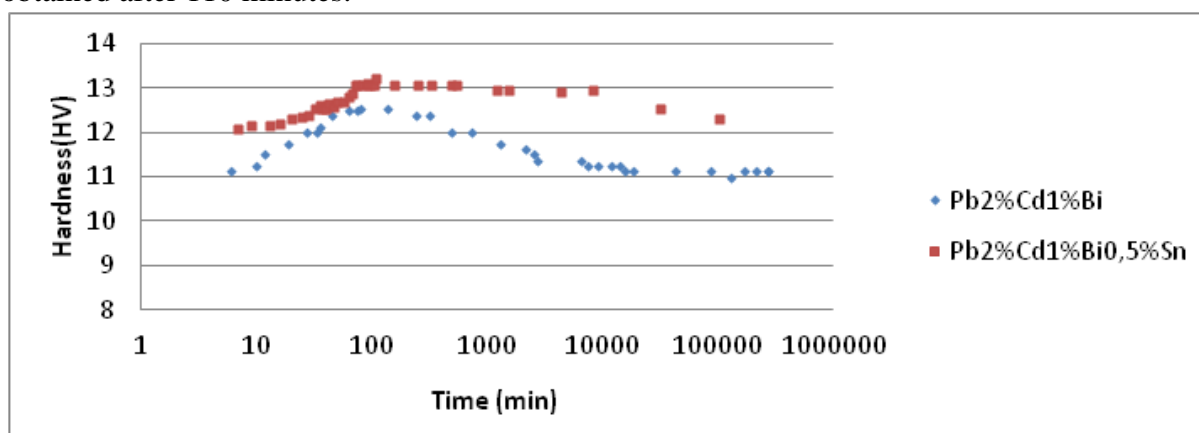


Fig. 4. Evolution of hardness versus time at 20 ° C for as-cast alloys Pb2%Cd1%Bi and Pb2%Cd1%Bi0,5%Sn.

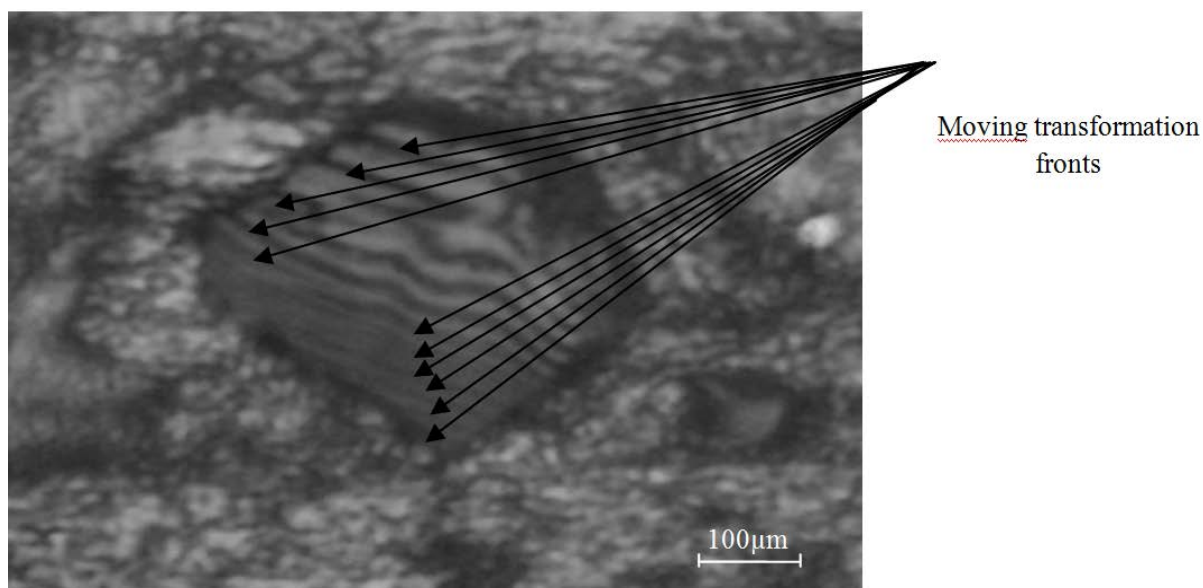
Similar to the alloy Pb2% Cd1% Bi [2], we followed the structure of the quenching alloy Pb2%Cd1%Bi0,5%Sn to the optical microscope, and we noticed that the same structural phenomena occur. Indeed, aging is characterized by a discontinuous transformation and hardening continuous reaction.

At 20 °C, the discontinuous transformation seems very retarded in the presence of tin; this is proved by the amplification of the hardness.

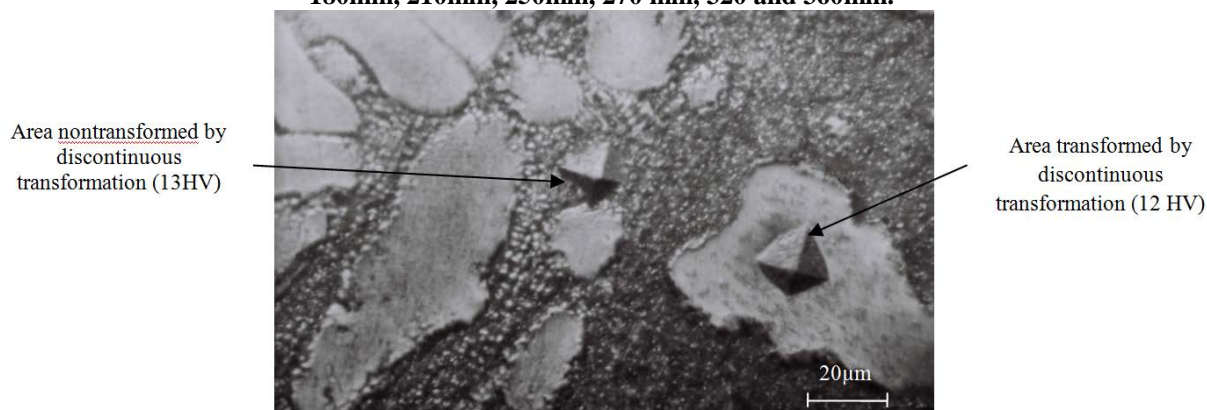
##### 3.1.2. Evolution of quenching structure of the as-cast alloy Pb 2% Cd1% Bi0, 5% Sn:

Fig. 5 shows the displacement of the fronts transformation at room temperature. Indeed, the addition of the tin reduces the progress of the transformation of fronts which reduces the speed of movement of these joints which explains the delay in the kinetics of the curing reaction.

Microhardness testing (Fig. 6) performed on this alloy in areas transformed by the discontinuous transformation and those nontransformed show that they are more hardened (about 13HV) and confirm that they are the seat of the continuous reaction.



**Fig. 5.** View of the movement of grain boundaries after successive chemical attack after quenching at 20 °C of the crude casting alloy Pb2% Cd1% Bi0,5% Sn for 15 min, 20 min, 50 min, 100 min , 150min, 180min, 210min, 250min, 270 min, 320 and 360min.



**Fig. 6.** Visualization of footprints of microhardness performed on the crude casting alloy Pb2% Cd1% Bi0, 5% Sn aged 50 minutes at 20°C.

For prolonged maintain at room temperature, the overaging occurs, it is characterized by the formation of large precipitates as shown in Figs. 7 and 8. Indeed, during overaging, the discontinuous precipitation softened alloy which consequently deteriorates the mechanical properties (Fig. 4).

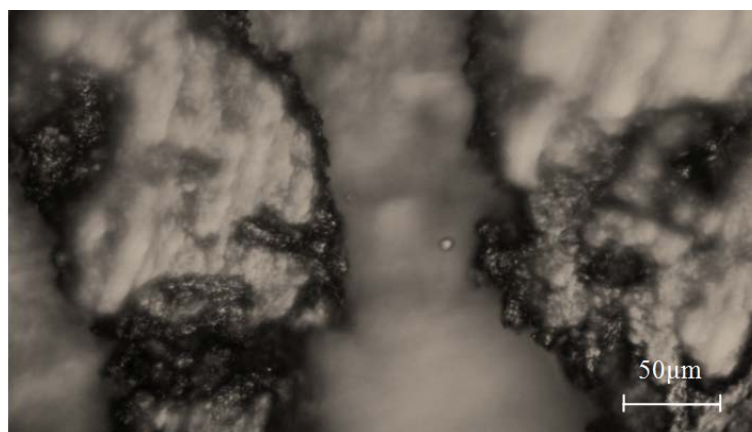


**Fig. 7.** View of the discontinuous precipitation of as-cast alloy Pb 2% Cd 1% Bi 0.5% Sn soaked in water at 20 °C after 7 hours and 6min.

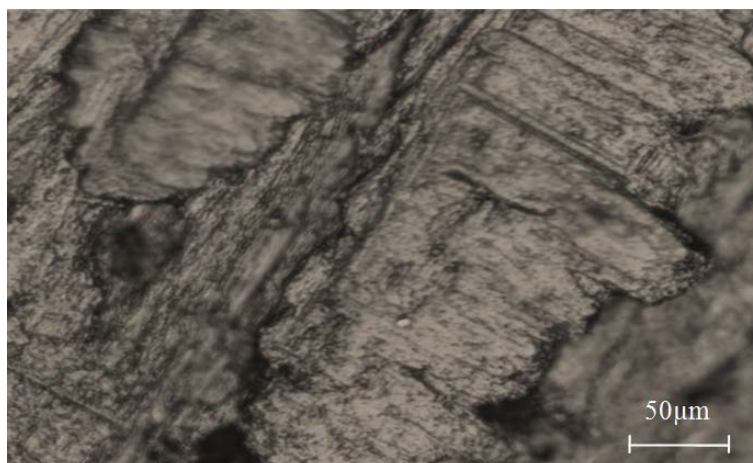


**Fig. 8.** View of the discontinuous precipitation of as-cast alloy Pb 2% Cd 1% Bi 0.5% Sn soaked in water at 20 °C after 2 days.

### 3.2. INFLUENCE OF THE HOLDING TEMPERATURE (80 °C):

#### 3.2.1. Hardness

Fig. 9 shows the change in hardness versus time at temperatures 20 °C and 80 °C, of the crude casting alloy Pb2% Cd1% Bi0, 5% Sn. The supersaturated tempered alloy has a hardness of 12.08 HV which is almost double than the pure lead whose hardness varies between 4 HV and 5 HV, which proves that the alloy is partially transformed during cooling. At 20 °C; the maximum hardness is 13.23 HV and is reached after 110 min, then the hardness slightly decreased to 12.50 HV beyond a month. At 80°C, the maximum hardening is reached within 102 min (~14 HV), after 18 hours we see a stagnation of hardness that decreases slightly to peak after 3 weeks 12 HV during aging.

Furthermore, the kinetics of the hardening process at 80°C (ripening temperature of battery plates and extreme operating temperature of a battery) appears similar relative to the room temperature except that there's a small increase in hardness.

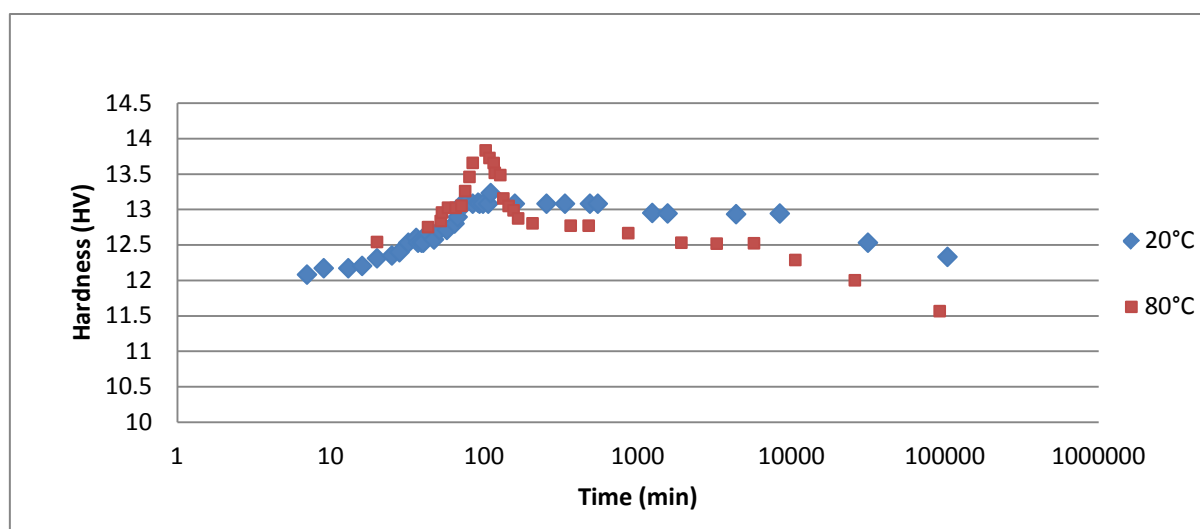


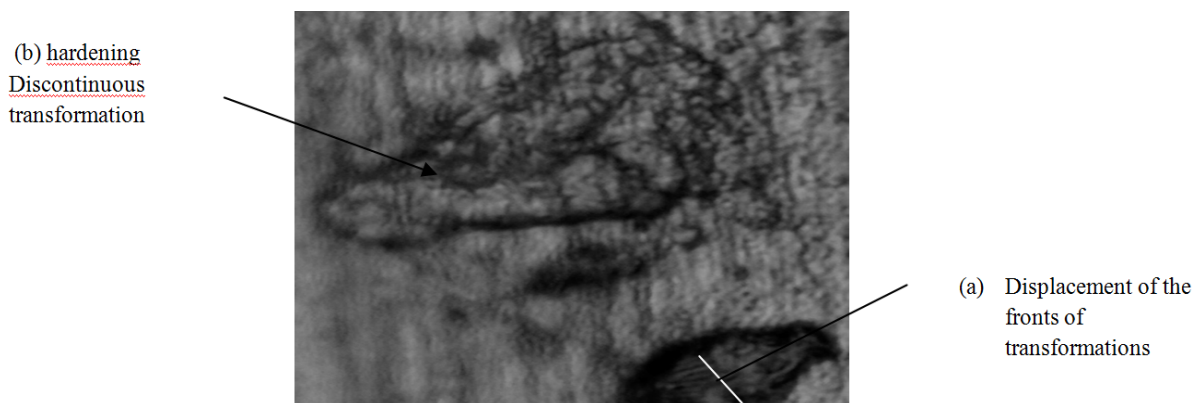
**Fig. 9.** Evolution of the hardness of as casting alloy Pb2% Cd1% Bi0, 5% Sn at temperatures 20°C and 80°C as a function of time.



### 3.2.2. Evolution of quenching structure of the alloy Pb 2% Cd1 %Bi0, 5% Sn (80 ° C)

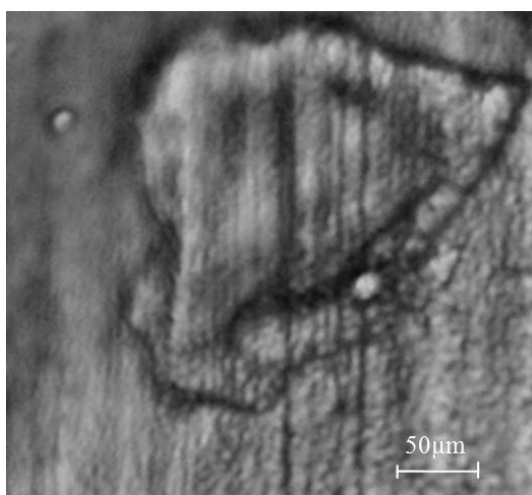
The structure of the alloy Pb 2% Cd1% Bi0,5% Sn at 80°C appears similar to that of 20 °C. In fact, the diffusion of the solute is made either homogeneously with the matrix; in this case it is a continuous transformation; or by a discontinuous processing mechanism which propagates along a front transformation often initiated at a grain boundary separating the transformed matrix of the initial matrix.

Figure 10-a shows the displacement of the fronts of transformation of the alloy Pb2% Cd1% Bi0,5% Sn maintained at 80 °C and figure 10-b shows the hardening discontinuous transformation of the same alloy during aging.



**Fig. 10. (a) Visualization of the movement of grain boundaries after successive chemical attack after quenching and holding at 80 °C of the alloy Pb2% Cd1% Bi0,5% Sn after 80 min of quenching (b) discontinuous Transformation of the alloy Pb2% Cd1%Bi0,5% Sn maintained at 80 ° C after 35min during aging.**

Figs. 11 and 12, shows the discontinuous precipitation during the overaging of the alloy Pb2%Cd1%Bi0,5%Sn. Indeed; the discontinuous precipitation deteriorates the mechanical properties which causes the softening of the material, it has been proved not only by the optical microscope, but also by the hardness (Fig. 4) and microhardness (Fig. 6).



**Fig. 11. View of the discontinuous precipitation of crude casting alloy Pb 2%Cd 1% Bi 0.5% Sn quenched with water and maintained at 80 °C after 3days of quenching during the overaging.**

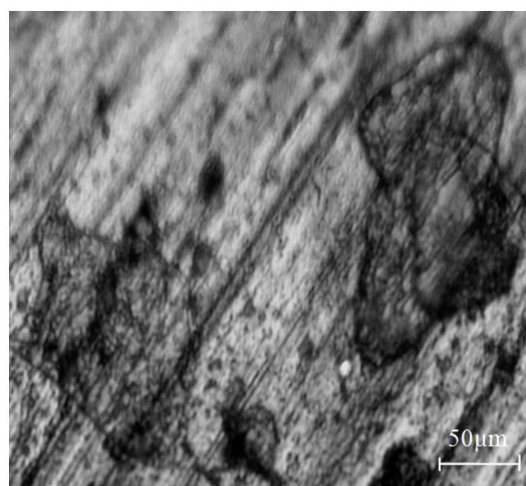


**Fig. 12. View of the discontinuous precipitation of crude casting alloy Pb 2%Cd 1% Bi 0.5% Sn quenched with water and maintained at 80 °C after 2 days and 20 hours of quenching during the overaging.**



### 3.3. INFLUENCE OF TIN

To study the influence of tin on the structural hardening mechanisms PbCdBiSn alloys, we worked on four different compositions. We have chosen the alloy whose hardness is maximal by referring to SAISSI and all [2]; it is Pb2% Cd3% Bi. We obtained the hardness curves shown in Fig. 13.

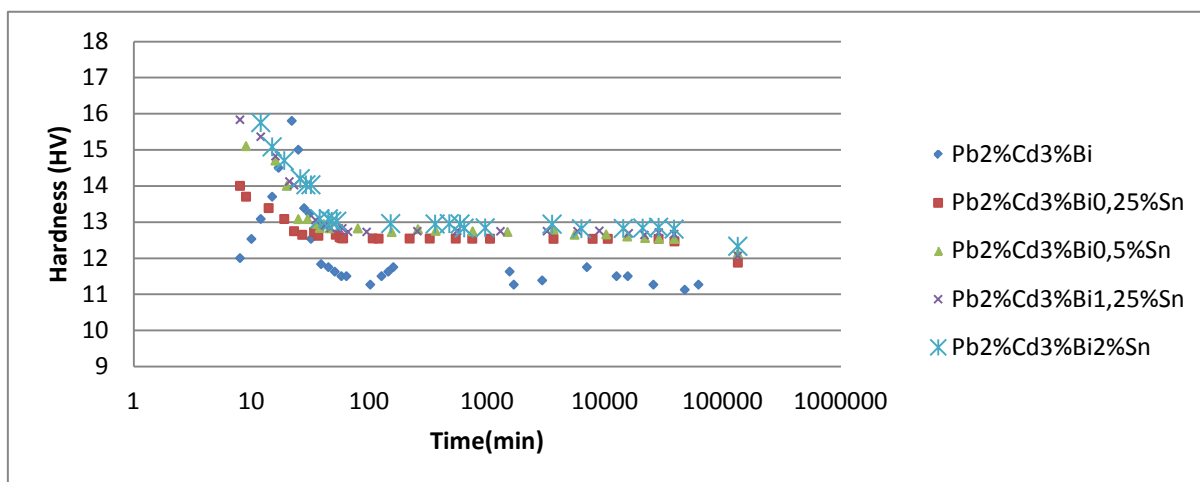


**Fig. 13. Evolution of the hardness versus time at room temperature of crude casting alloys Pb2%Cd3%Bi; Pb2%Cd3%Bi0, 25%Sn et Pb2%Cd3%Bi0,5%Sn, Pb2%Cd3%Bi1,25%Sn et Pb2%Cd3%Bi2%Sn.**

According to Fig. 13, we have not been able to visualize the aging of alloys in the presence of tin; this is probably due to the presence of a high concentration of bismuth which is consistent with the results found previously [1] and [2]. Indeed, bismuth accelerates the hardening reaction and slightly increases the hardness, tin also increases hardness and during overaging we note that the curves are similar for different proportions of tin with a slight increase of hardness of about 1HV as shown in Fig. 13. For further visualization of the influence of tin we decreased the percentage of bismuth, and studied the alloy Pb2% Cd2% Bi. The results are shown in Fig. 14.

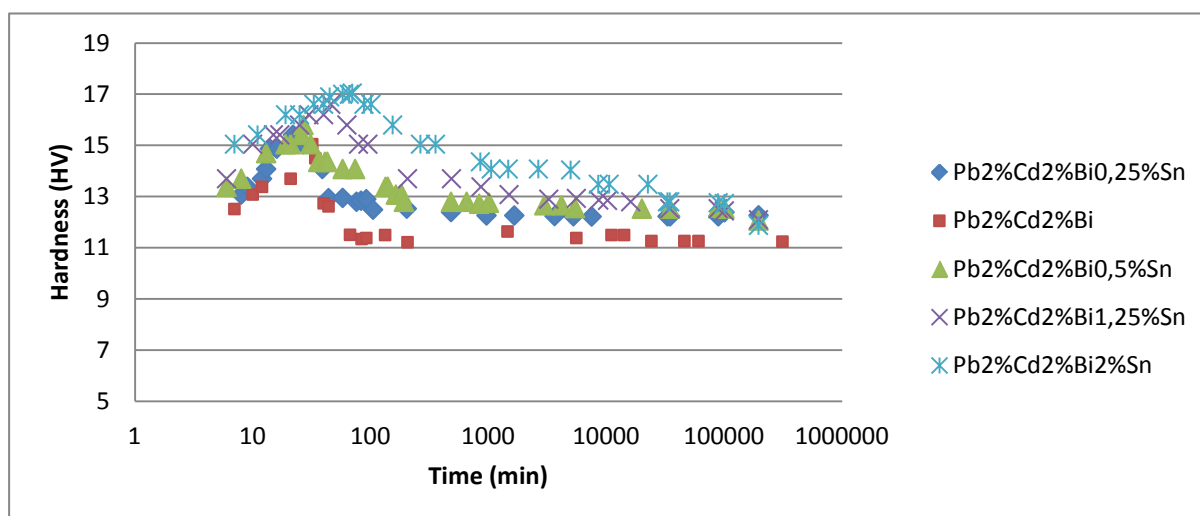


**Fig. 14. Evolution of the hardness versus time at room temperature of crude casting alloys Pb2%Cd2%Bi; Pb2%Cd2%Bi0, 25%Sn et Pb2%Cd2%Bi0, 5%Sn, Pb2%Cd2%Bi1, 25%Sn et Pb2%Cd2%Bi2%Sn.**

According to Fig. 14, a low content of tin (0.25% Sn and 0.5% Sn) does not delay the hardening reaction compared to high levels of tin (1.25% Sn and 2% Sn), this is due to the presence of bismuth. Indeed, progressively as the concentration of tin increases, the aging process seems more delayed.

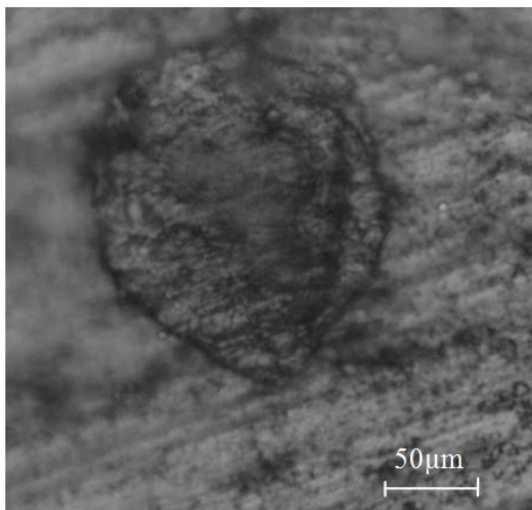


**Fig. 15. Visualization of the discontinuous precipitation of the crude casting alloy Pb 2% Cd 2% Bi 0, 25%Sn quenched with water after 4 hours of quenching during the overaging.**

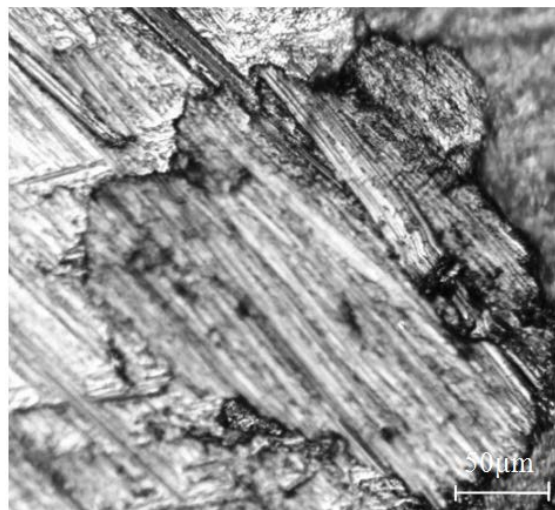


**Fig. 16. Visualization of the discontinuous precipitation of the crude casting alloy Pb 2% Cd 2% Bi 0,5%Sn quenched with water after 1 day of quenching during the overaging.**

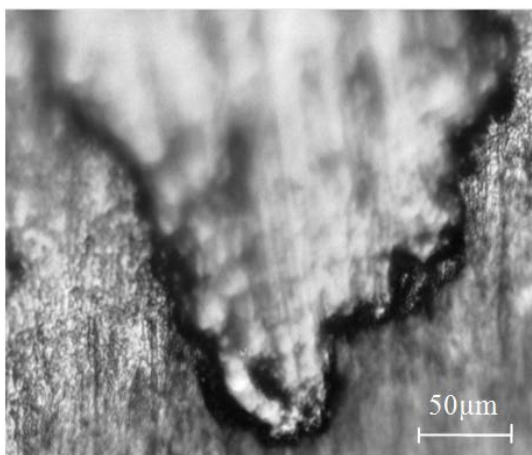


**Fig. 17. Visualization of the discontinuous precipitation of the crude casting alloy Pb 2% Cd 2% Bi 1, 25%Sn quenched with water after 5 hours of quenching during the overaging.**

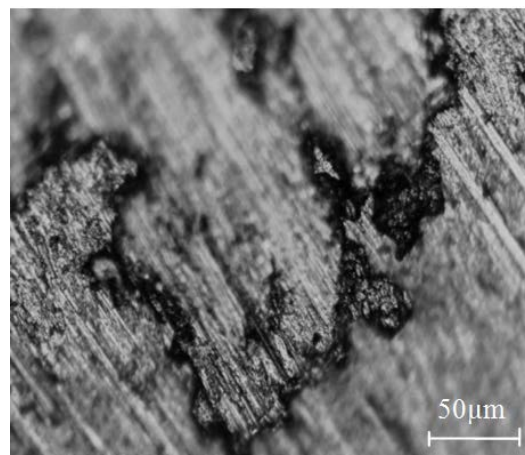


**Fig. 18. Visualization of the discontinuous precipitation of the crude casting alloy Pb 2% Cd 2% Bi 2%Sn quenched with water after 2 hours of quenching during the overaging.**

According to Figs. 15, 16, 17 and 18, the same structural transformations appear when overaging, these transformations take a little longer to appear. This is due to the competition between the tin and bismuth, the first being a self timer and the second an accelerator.

### 3.4. INFLUENCE OF REHOMOGENIZATION

Fig. 19 shows the evolution of the hardness as a function of time at room temperature of raw casting and rehomogenized alloys quenched with water. Globally the rehomogenized alloys age in the same way as the raw casting except that aging seems more accelerated.

Indeed, rehomogenization process reduces, by diffusion, the heterogeneity of composition due to segregation phenomena which appear in the solidification structure which lets understand that reducing initiation sites of the discontinuous transformation amplifies hardness.

The maximum hardness of rehomogenized samples (14, 16 HV) is higher than that of the raw casting samples (13,23HV). This is due to the dissolution of segregated phase during the treatment of rehomogenization, which increases the supersaturation after quenching at 20°C.

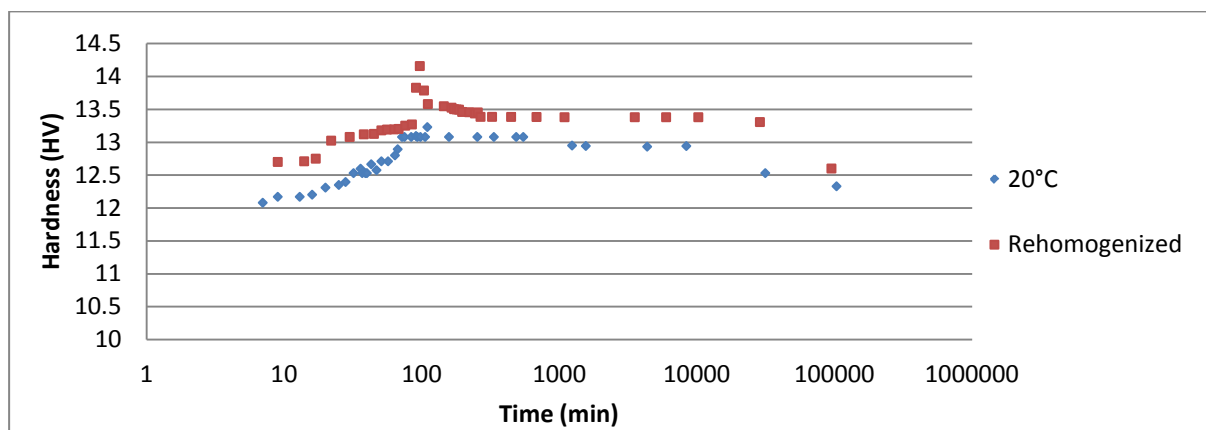


Fig. 19. Evolution of hardness as function of time at 20°C, for alloy Pb2%Cd1%Bi0,5%Sn, as-cast and rehomogenized and then soaked in water.

Microscopic observations (Fig. 20) show that the structural hardening mechanisms of rehomogenized alloy are similar to those of the as-cast alloy, the aging effect is characterized by a discontinuous processing and a hardening continuous reaction, and overaging is characterized by softening discontinuous precipitation.

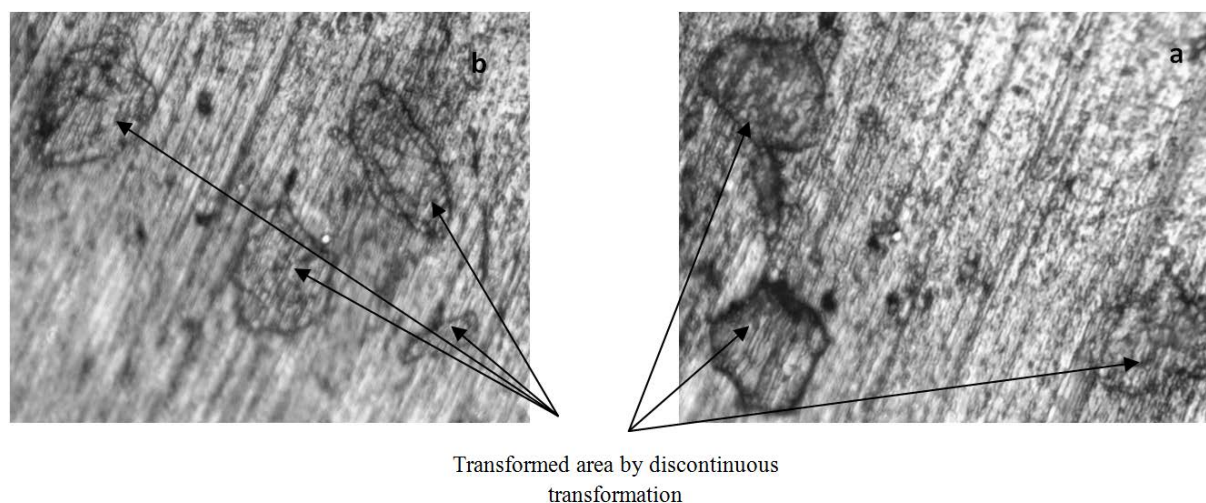


Fig. 20. a) Visualization of the discontinuous processing of rehomogenized alloy Pb 2% Cd 1% Bi 0,5%Sn after 60 minutes of quenching at 20 °C. b) Visualization of the discontinuous processing of rehomogenized alloy Pb 2% Cd 1% Bi 0,5%Sn after 3 days of quenching at 20 °C.

## 4. X-RAY DIFFRACTION ANALYSIS

### 4.1. INTERPRETATION OF THE RESULTS OF THE XRD ANALYSIS FOR THE SAMPLE Pb2% Cd2% Bi0, 5% Sn

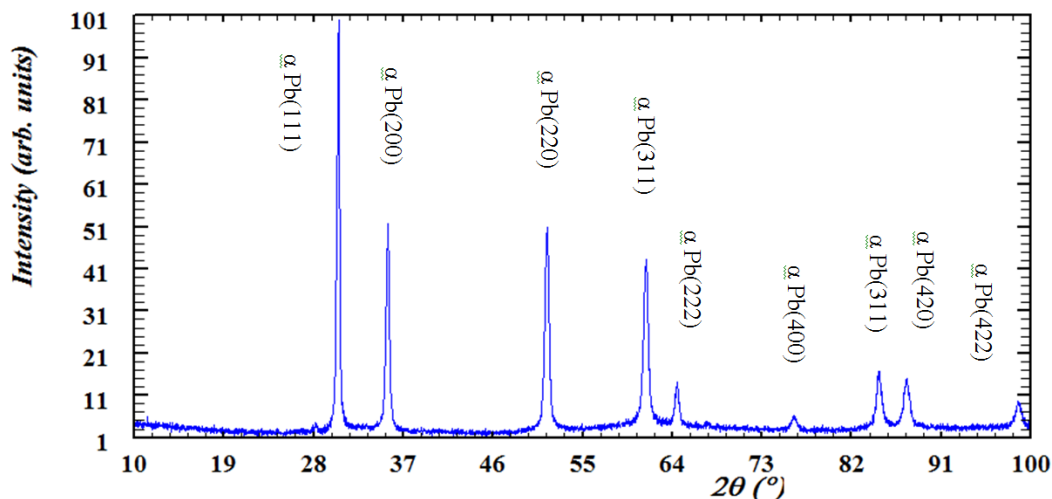


Fig. 21. X-ray diffraction analysis of the surface of the alloy Pb2%Cd2%Bi0,5%Sn.

According to the X-ray diffraction diagram of Fig. 21, the treatment of diffractograms or specters of the alloy Pb 2% Cd 2% Bi0, 5% Sn, highlights the peaks of the solid solution  $\alpha$  lead, which crystalline structure is CFC.

Table 2. Crystallographic parameters of the alloy Pb 2% Cd2% Bi0, 5% Sn.

$2\theta$ [13]	$2\theta$ calculated	$d_{hkl}$	hkl	Parameter a
31.270	30.50422	2.92257	111	5.05
36.262	35.46926	2.52321	200	5.04
52.220	51.44650	1.77122	220	5.00
62.139	61.37566	1.51206	311	5.00
65.233	64.49796	1.43983	222	4.95
76.985	76.14977	1.24865	400	4.96
85.416	84.77147	1.13818	331	4.92
88.189	87.62082	1.10844	420	4.91
99.334	98.73341	1.01922	422	4.89

### 4.2. INTERPRETATION OF THE RESULTS OF THE XRD ANALYSIS FOR THE SAMPLE Pb2% Cd2% Bi1,2 5% Sn

According to the X-ray diffraction diagram of Fig. 22, the treatment of diffractograms or specters of the alloy Pb 2% Cd 2% Bi1,25% Sn, highlights the peaks of the solid solution  $\alpha$  lead, which crystalline structure is CFC.

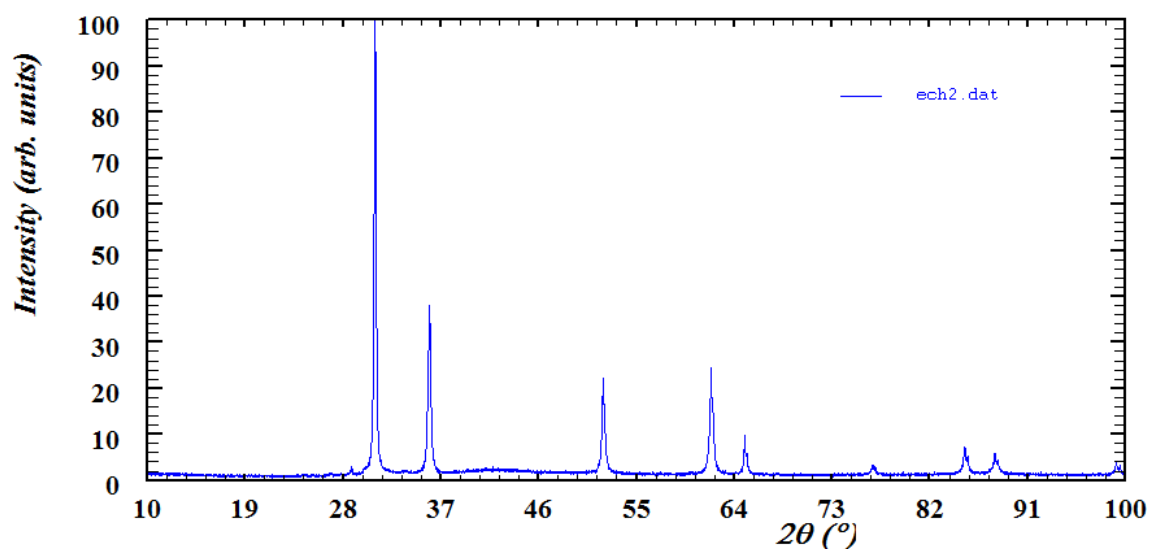


Fig. 22. X ray diffraction analysis of the surface of the alloy Pb2% Cd2 %Bi1, 25% Sn.

Table 3. Crystallographic parameters of the alloy Pb 2% Cd2% Bi1, 25% Sn.

2θ [13]	2θ calculated	d <sub>hkl</sub>	hkl	Parameter a
31.270	30.95723	2.88789	111	4.98
36.262	35.95356	2.49596	200	4.98
52.220	51.94234	1.75512	220	4.94
62.139	61.87592	1.49703	311	4.94
65.233	64.97247	1.42533	222	4.91
76.985	76.74722	1.23893	400	4.92
85.416	85.20323	1.13378	331	4.92
88.189	88.09879	1.10510	420	4.91
99.334	99.33086	1.00951	422	4.89

#### 4.3. INTERPRETATION OF THE RESULTS OF THE XRD ANALYSIS FOR THE SAMPLE Pb2% Cd2% Bi2% Sn

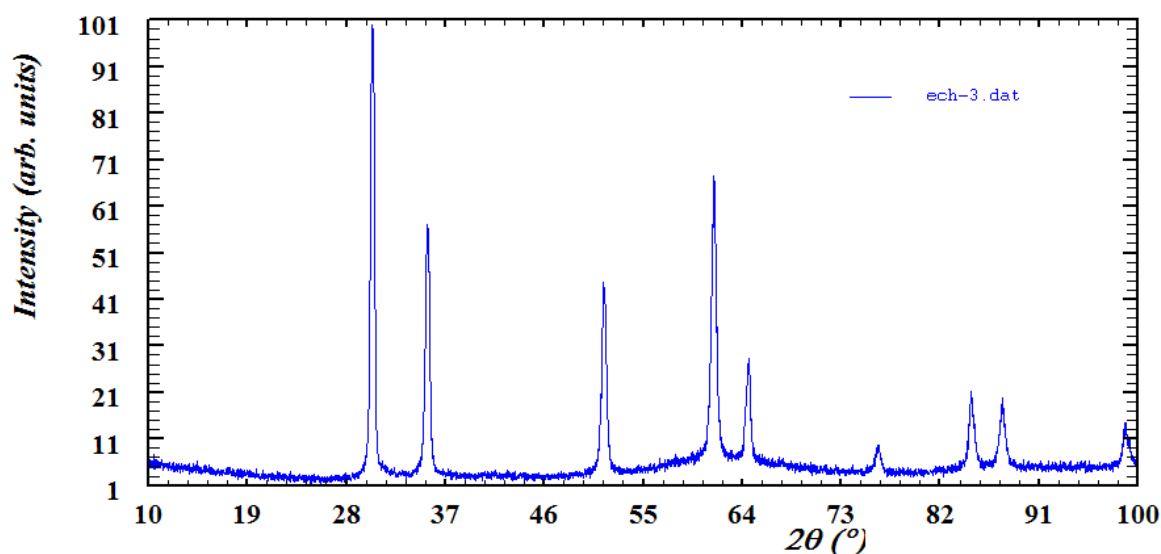


Fig. 23. X ray diffraction analysis of the surface of the alloy Pb2% Cd2 %Bi2%Sn.

According to the X-ray diffraction diagram of Fig. 23, the treatment of diffractograms or specters of the alloy Pb 2% Cd 2% Bi2% Sn, highlights the peaks of the solid solution  $\alpha$  lead, which crystalline structure is CFC.

**Table 4. Crystallographic parameters of the alloy Pb 2% Cd2% Bi2% Sn.**

<b>2<math>\theta</math> [13]</b>	<b>2<math>\theta</math> Calculated</b>	<b>d<sub>hkl</sub></b>	<b>hkl</b>	<b>Parameter a</b>
31.270	30.38178	2.94432	111	5.09
36.262	35.37856	2.53805	200	5.06
52.220	51.45253	1.77331	220	5.00
62.139	61.44253	1.51641	311	5.00
65.233	64.57139	1.43874	222	4.95
76.985	76.38874	1.24756	400	4.96
85.416	84.83845	1.14599	331	4,96
88.189	87.70314	1.11014	420	4.96
99.334	98.97239	1.00858	422	4.89

The diagrams of X-ray diffraction of the alloys Pb2%Cd2%Bi0,5%Sn, Pb2%Cd2%Bi1,25%Sn and Pb2%Cd2%Bi2%Sn (Figs. 21 - 23), visualize only the peaks of the solid solution  $\alpha$  lead, which crystal structure is a cubic face-centered.

However, we can not say that the precipitation of secondary phases has not happened; the deduction we can make is that the X ray diffraction could not bring out such precipitation and those; seen their small size compared to that of lead.

#### 4.4. COMPARISON OF DIFFRACTION PEAKS DURING OVERAGING

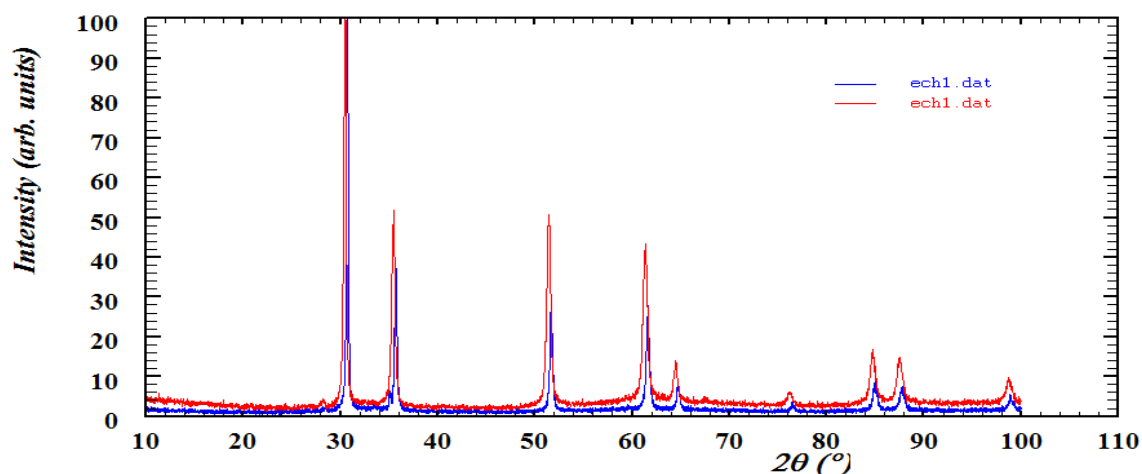


**Fig. 24. Comparison of the peaks of the alloy Pb2%Cd2%Bi0,5%Sn via X-ray diffraction through time.**



**Table 5. Peak intensities of the alloy Pb2%Cd2%Bi2%Sn after 6 months and 9 months of quenching.**

Peak intensity after 6 months of aging	Peak intensity after 9 months of aging
99,972	100,12
38,142	51,847
28,543	50,718
27,696	42,813
9,3450	14,298
3,3450	6,3924
9,0627	16,839
7,9334	15,145
5,6748	9,7804

Gradually, as time increases, the intensity increases more as shown in Fig. 24 and Table 4, this proves the decrease of hardness hence softening.

Indeed, when the alloy tends toward equilibrium, there is a rearrangement of atoms these; becoming more intense even more crystallized, influences bad on mechanical properties making them deteriorated.

## 5. CONCLUSION

The structural hardening of the alloy Pb-Cd-Bi-Sn is experiencing the same phenomena than the alloy Pb-Cd-Bi already studied [2]. Indeed, the discontinuous transformation and hardening continuous reaction are the competitive structural mechanisms causing in sequence to the time scale during aging, while the over-aging is characterized by a softening discontinuous precipitation which precipitate is cadmium.

Alloys containing tin has shown a change of hardness compared to those free of tin. Indeed, as the tin content increases, the hardness increases further and the kinetics of the hardening reaction occurs slowly. However, bismuth being an accelerator of the continuous reaction is in competition with tin, which influences the speed of aging.

The structural hardening process for rehomogenized alloys are identical to those of the raw casting alloys but the kinetics of aging seems more accelerated, thus entailing an increase of the hardness. The dissolution of the segregated phases during the treatment of rehomogenization increases the supersaturation after quenching by eliminating segregation cells in the solidification structure which are the priming area of the discontinuous processing.

Besides lead, the results of analyzes by X-ray diffraction, were not able to show the other elements of the alloy, this is due to their very low compositions. In addition, as the time increases the intensity also increases which leads to a deterioration of mechanical properties since the alloy tends towards equilibrium. We also determined the crystal structure parameters of the quaternary alloys PbCdBiSn.

At last, comparison of the hardness values obtained by the quaternary alloys PbCdBiSn to those given by the ternary alloys PbCdBi shows the beneficial effect of tin additions on the mechanical properties of these alloys. Indeed, given that bismuth is an accelerator, we could not know the maximum hardness for alloys Pb2% Cd3% Bi0, 25% Sn, 0.5% Sn, 1.25% Sn and 2% Sn, knowing that the same alloy without tin peaked 16 HV. But it is strongly observed that all of the maximum hardness values obtained were higher in the presence of tin. Thus, the improvements brought by the addition of tin in mechanical properties, lets say that the alloys highly charged of tin are favorable to industrial development.



## 6. REFERENCES

- [1] Bouirden, L., *Thèse de doctorat de 3ème cycle*, Nancy 1990.
- [2] Saissi, S., et al, *Journal of Science and Arts*, **4**(29), 331, 2014,
- [3] Massalski, T.B., *Binary phase diagrams*, second Edition, ASM International, 1990.
- [4] Karakaya, I., Thompson, W.T., *International ASM Handbook*, 1988.
- [5] Osamura, K., Du, Z., *Journal of Phase Equilibria*, **14**, 206 1993.
- [6] Okamoto, H., *ASM volume 3: Alloy phase diagrams*, 1990.
- [7] Hansen, M., Anderko, K., *Constitution of Binary Alloys*, McGraw-Hill, New York, 2<sup>nd</sup> ed., 1958.
- [8] Elliot, R.P., *Constitution of Binary Alloys*, 1st Suppl., McGraw-Hill, New York, 1965.
- [9] Shunk, F.A., *Constitution of Binary Alloys*, 2<sup>nd</sup> Suppl., McGraw-Hill, New York, 1969.
- [10] Moffatt, M.G., *The Handbook of Binary Phase Diagrams*, General Electric Co., Genium Publishing Corporation, Schenectady, NY, USA (continuous updating).
- [11] Massalski T.B., *Binary Phase Diagrams*, American Society for Metals, International Materials Park, OH, USA, 2<sup>nd</sup> ed., 1990.
- [12] Hilger, J.P., *Métallographie du plomb et de ses alliages, cours de formation intensive de courte durée COMETT Nancy*, textes rassemblés et édités par Hilger J.P.: Laboratoire de thermodynamique Métallurgique, Université de Nancy I, N° ISBN: 29505658-2-0, pp 1-14.
- [13] Wyckoff, R.W.G., *Crystal Structures*, **1**, 7, 1963.